DOI: 10.1007/s12541-012-0212-2

Damage Prediction in the Multistep Forging Process of Subminiature Screws

Jong-Bong Kim[1], Won-Sang Seo[2], and Keun Park[3,#]

1 Dept. Mech. Automotive Engng., Seoul National University of Science and Technology, Seoul, Republic of Korea, 139-743
2 Graduate Sch. of NID Fusion Tech., Seoul National University of Science and Technology, Seoul, Republic of Korea, 139-743
3 Dept. Mech. System Design Engng., Seoul National University of Science and Technology, Seoul, Republic of Korea, 139-743
Corresponding Author / E-mail: kpark@seoultech.ac.kr, TEL: +82-2-970-6358, FAX: +82-2-974-8270

KEYWORDS: Cold forging, Precision screw, Damage, Crack, Finite element analysis

In this study, a multi-step forging process of subminiature Torx screws is investigated. The production of subminiature screws requires precision forming technologies for the head forging process and the thread rolling process. In the head forging process, various defects such as micro-cracks or material folding are frequently observed due to the small size of screw heads and the highly-concaved geometry of the Torx pattern. To predict the formation of these defects, finite element (FE) analyses were performed for the multistep forging process of subminiature screws. The Cockcroft-Latham damage criterion was used to predict micro-cracks and the refined mesh was used to predict the folding defect, from which the possibilities of the crack and folding defects were numerically evaluated. Based on the FE analysis results, the effects of die design parameters and forging conditions were investigated for the purpose of reducing the amount of defects. The design of multistep dies was changed and analyzed through FE simulation. Experiments based on the analysis results were conducted, and the improved die can be used to prevent the formation of crack defects and folding defects.

Manuscript received: October 30, 2011 / Accepted: April 13, 2012

NOMENCLATURE

H_I = initial specimen length corresponding to a screw head
H_M = height of a preformed screw head
H_F = height of a final screw head
R = curvature radius of an upper die for preform forging
FR = forging ratio
$\bar{\varepsilon}$ = effective plastic strain
$\bar{\sigma}$ = effective stress
σ_1 = principal stress
C = Cockcroft-Latham damage value

1. Introduction

Screws are used to join the various electronic products and machines. Recent trends in the miniaturization and weight reduction of portable electronic parts have boosted the use of subminiature screws. Subminiature screws can be characterized by the small diameter, less than 3 mm in general, and micrometer-scale pitch. The subminiature screw must have a sufficient torque transmission capacity in spite of its small size. Thus, Torx (*) head screws[1] are popularly used instead of the conventional cross (+) head screw when high-torque transmission capacity is required for subminiature screws. The Torx screw is characterized by its head pattern shaped like a six-point star (*).

Metal screws are usually manufactured in two processes: a head forging process and a thread rolling process. In the head forging process, a rod-type workpiece is forged to shape the screw head, including its pattern. In the case of a Torx head screw, defects such as micro-cracks or folding tend to form due to the screw's unique star-shaped pattern.[2] The small size of the subminiature screw head could also be a reason for these defects during the forging process. These defects may dramatically reduce the joining torque of a screw.

To predict defects in the forging process, finite element (FE) analysis is widely used.[3,4] An FE analysis of the forging process requires automatic remeshing because large deformations during the simulation tend to distort the mesh.[5] Predicting material folding defects requires special numerical schemes, such as adaptive mesh refinement and contact treatment. Predicting cracks in the forging process generally involves the use of numerical damage models.[6,7]

In this study, two major defects (cracks and folding) that occur in the forging process of subminiature Torx screws are predicted by

FE analysis. Based on the authors' previous works,[2] two-step forging process was used to reduce the formation of cracks. The effects of die design parameters and processing conditions were also investigated in order to minimize defects. The design changes for multistep dies were then analyzed and optimized through FE simulations and verified by means of experimental comparison.

2. Overview of the Multistep Forging Process

2.1 Process overview

In this work, a two-step head forging process for a subminiature Torx screw is concerned. Figure 1 shows the configuration of an M2.6 Torx screw: the major diameter is 2.6 mm, the pitch is 0.45 mm, the diameter of the head is 5.3 mm, and the thickness of the head is 1.6 mm. The head of the screw was formed from a long rod with a diameter of 2.5 mm. The area ratio of the head forging is 4.49, which is sufficiently large to result in the forging defects because severe material deformation is required.

The forging load and defects are generally reduced by means of a screw heading process that consists of an intermediate forging stage and a final forging stage.[2] In the intermediate forging stage, a preform is formed as an intermediate shape between the initial billet and the final product. The final forging stage is then performed along with the indentation of the Torx pattern. Figure 2 shows the configuration of the two-step head forging processes, which includes the initial billet, the intermediate preform and the final product.

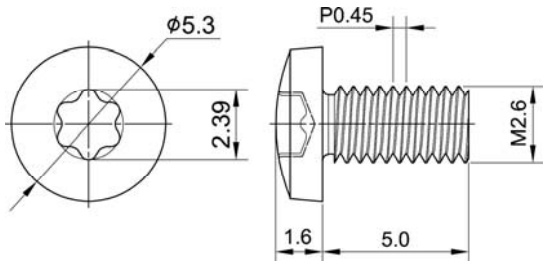

Fig. 1 Configuration and dimensions of a subminiature screw (M2.6)

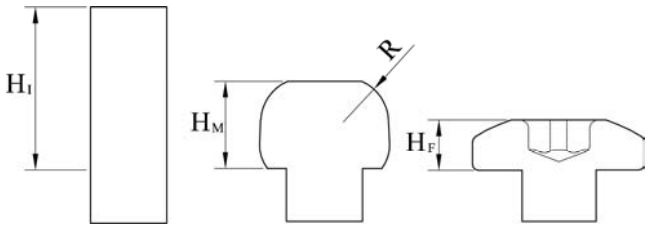

Fig. 2 Configuration of the two-step head forging processes: (a) the initial billet, (b) the intermediate preform and (c) the final product

Fig. 3 Two major defects in the screw head forging process[2]

Figures 3 (a) and (b) show two major defects in the screw head forging process: the micro-crack and folding defects, respectively. It can be seen that the crack was initiated at the concave part of the Torx pattern and developed to the outside radial direction. In contrast, the folding defects were observed inside the Torx pattern.

2.2 Consideration of the design parameters

The authors' earlier work confirmed that a modification of the top die for the preform forging can change the material flow characteristics and improve the crack and folding defects.[2] In this study, the effect of design parameters for the intermediate forging die is investigated.

Two design parameters are taken into account: the curvature radius of the upper die (R), which is marked in Fig. 2(b), and the preform forging ratio (FR). The FR is defined as follows:

$$FR(\%) = \frac{H_I - H_M}{H_I - H_F} \times 100 \quad (1)$$

where the parameters H_I, H_M, and H_F are illustrated in Fig. 2. To investigate the effect of these design parameters, we applied FE analysis to 16 cases: that is, a full factorial combination of four levels of the FR and four levels of R. Table 1 lists the details of the levels of each parameter.

The FE analyses were conducted with Deform-3D®, a commercial FE analysis code for metal forming processes. The workpiece was treated as a deformable body and the dies were modeled as a rigid body. Before conducting a parametric study, we investigated the element size effect and found that around 100,000 elements were used in the analysis.[2] To describe the material folding appropriately, the region near the Torx pattern was discretized with the refined mesh structure. The material properties of AISI SUS304 were adopted from the work of Chen and Young.[8]

3. FE Analysis of the Head Forging Processes

3.1 Prediction of crack defects

To evaluate the possibility of the crack defects, the results of effective stress and effective plastic strain are discussed. Figures 4(a) and 4(b) show the distributions of the effective stress and strain at the final forging stage (FR=80 %, R=1.5 mm). It can be seen that the location of the maximum effective stress is not remarkable to be

Table 1 Two design parameters with four levels

Level	Design parameters	
	Forging ratio (FR)	Corner radius (R)
1	80.0 %	3.0 mm
2	85.1 %	2.0 mm
3	88.8 %	1.8 mm
4	95.3 %	1.5 mm

regarded as the location of crack initiation, as shown in Fig. 4(a). On the other hand, the maximum effective strain is located on the bottom of Torx shape as shown in Fig. 4(b), which is quite different from the experimentally observed crack location in Fig. 3(a).

Thus, the crack initiation is predicted by using the Cockcroft-Latham (C-L) damage theory in this study. The C-L damage prediction model during plastic deformation is defined as[9]

$$\int^{\bar{\varepsilon}} \frac{\sigma_1}{\bar{\sigma}} d\bar{\varepsilon} = C \tag{2}$$

where σ_1 is the principal stress, $\bar{\varepsilon}$ is the effective plastic strain, and $\bar{\sigma}$ is the effective stress. This C-L damage model regards that a crack initiates when the maximum principal stress reaches to a critical value. This model evaluates the order of damage value (C) by calculating the amount of the critical plastic work as defined in Eq. (2). To predict the crack initiation accurately, the critical C value should be calibrated on the basis of the experimental results under various stress conditions. In this study, the C-L damage value is used as a relative measure for the possibility of the crack initiation instead of a direct prediction.

Figures 5(a) to 5(d) show the predicted damage distributions with variations of the forging ratio (F) and the curvature radius (R). The overall damage values decrease as the FR increases and the curvature radius of the upper die for the preform decreases. The damage value is large in two regions: the region near the concave part of the Torx pattern (marked as A) and the region near the outermost periphery (marked as B).

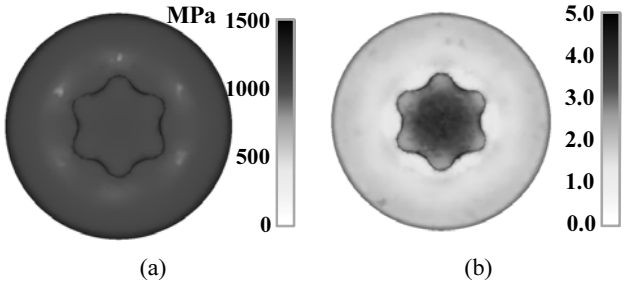

(a) (b)

Fig. 4 (a) Effective stress (unit: MPa) and (b) effective plastic strain at the end of heading process (FR = 80 %, R = 1.5 mm)

Table 2 Damage values after the final forging in region A for various values of FR and R

R \ FR	80 %	85 %	89 %	95 %
3.0 mm	0.47	0.45	0.42	0.40
2.0 mm	0.43	0.43	0.37	0.31
1.8 mm	0.42	0.41	0.36	0.30
1.5 mm	0.38	0.35	0.32	0.27

Table 3 Damage values after the final forging in region B for various values of FR and R

R \ FR	80 %	85 %	89 %	95 %
3.0 mm	0.36	0.36	0.34	0.34
2.0 mm	0.36	0.36	0.34	0. 34
1.8 mm	0.34	0.36	0.34	0. 33
1.5 mm	0.35	0.37	0.34	0. 34

The damage values with various FR and R values are summarized in Table 2 (for region A) and Table 3 (for region B). Clearly, the peak damage value at region A decreases as the value of FR increases and the value of R decreases. Therefore, a large FR value and a small R value are recommended for reducing the possibility of crack initiation. The damage values in region B, however, indicate a relatively low level of deviation for all cases. This observation can be explained by the fact that the material flow displays rotationally symmetric behavior in region B. In this case, the principal stress is mainly a function of the principal strain; it can be expressed as follows:

$$\varepsilon_1 = \ln(r / r_0) \tag{3}$$

Figure 6 shows the damage distributions along the AB line (of Fig. 5(a)), representing that the damage values in regions A and B are larger than the damage values at the midpoint. When FR is 80%, the damage value in region A is greater than the damage value in region B. These results indicate that a crack initiates in region A

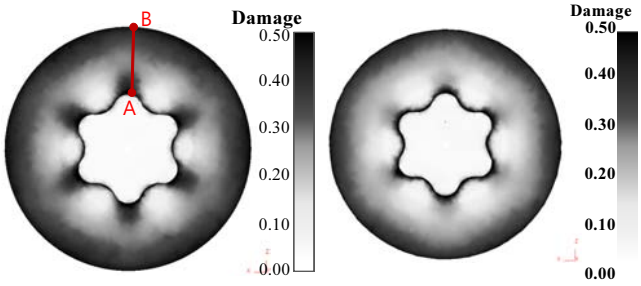

(a) FR = 80%, R = 3.0 mm (b) FR = 95%, R = 3.0 mm

(c) FR = 80%, R = 1.5 mm (d) FR = 95%, R = 1.5 mm

Fig. 5 Comparison of the damage value distribution for different values of FR and R

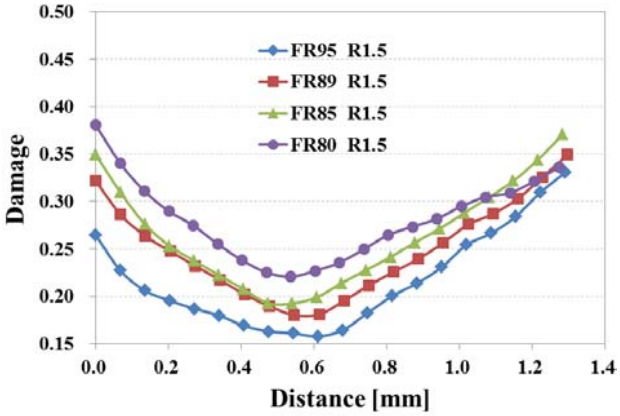

Fig. 6 Damage value distributions along the AB line

rather than in region B. As the FR increases, however, the damage value in region A decreases whereas the damage value in region B remains almost the same. In contrast, the damage value in region A becomes lower than that in region B when the FR is 95%, which means a crack is more likely to be initiated in region B than in region A.

Figure 7 shows the damage evolution during the second forging stage at four different points (P_1 to P_4). In this graph, the stroke was taken to be the last millimeter for each condition because the overall stroke varies in relation to the FR value. The damage value at P_1, near the Torx pattern, sharply increases in the early stage of the final heading process. The damage value at P_4, however, continually increases. These results indicate that a crack may be initiated near the Torx pattern (P_1) in the early stage of the head forging process.

3.2 Prediction of folding defects

In this section, we use FE analyses to investigate folding detects. An FE analysis was performed for the initial condition (FR=80%, R=3.0 mm). Figure 8(a) shows a shaded image of the finally formed shape. A region of discontinuous color inside the Torx pattern is marked and enlarged. The discontinuous color, which originates from irregularly shaped elements near the corner region, is due to a folding defect. The sectional view in Fig. 8(b) shows the shape in more detail near the corner of the pattern. Several discontinuous profiles can be observed; they are regarded as folding defects.

To investigate how design parameters affect folding defects, we conducted FE analysis on various FR and R values. The results, which are summarized in Table 4, show that there are no folding defects when the FR is 95%, regardless of the value of R. Therefore, it can be concluded that the curvature radius (R) has no effect on folding defects. Figure 9 shows a sectional view of the finally formed shape when the FR and R values were set at 95% and 3.0 mm, respectively. The corner region has a smooth profile, which means there is no folding defect.

The material flows of two cases, that is, 80% FR and 95% FR, are compared in Figs. 10(a) and 10(b). Figure 10(a) shows that the material flows downwards to the folding region. This downward flow causes the folding defect by accumulating material. Figure 10(b) shows that the material flows outward and does not accumulate inside the Torx pattern. Because a high FR value tends to reduce the head thickness, the material flow near the pattern corner consequently changes from a downward direction to an outward direction, resulting in the prevention of any folding defects.

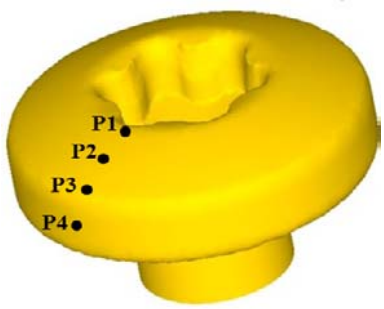

(a) Sample point locations

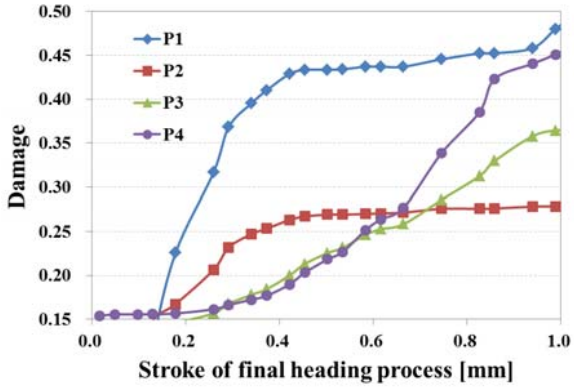

(b) Damage value changes

Fig. 7 Damage evolution during the final heading process (FR = 80%, R = 3 mm)

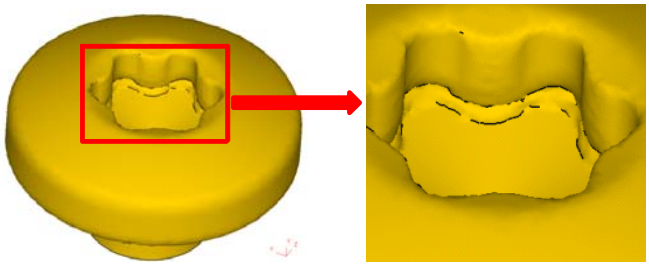

(a) Isometric view

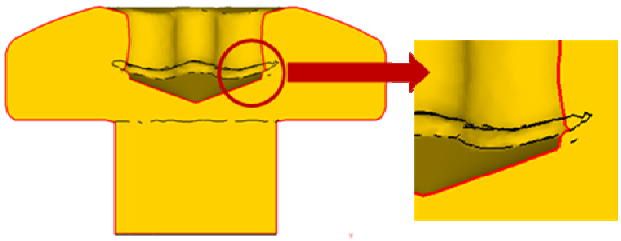

(b) Sectional view

Fig. 8 Predicted folding defect inside a Torx pattern (FR = 80%, R = 3.0 mm)

Table 4 Improvement of folding defects inside the Torx pattern for various values of FR and R (F: Folding, N: No folding)

R \ FR	80 %	85 %	89 %	95 %
3.0 mm	F	F	F	N
2.0 mm	F	F	F	N
1.8 mm	F	F	F	N
1.5 mm	F	F	F	N

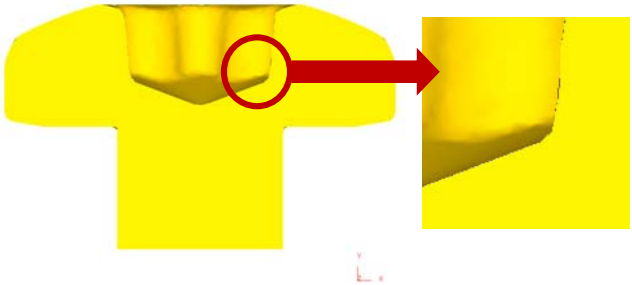

Fig. 9 Sectional view of the final shape without any folding defects (FR = 95 %, R = 3.0 mm)

4. Experimental Verification

Based on the results of the FE analyses, the forging ratio (FR) and the corner radius (R) were set to 9% and 1.5 mm, respectively. The die sets for the multistep forging were then fabricated, and forging experiments were performed with the initial die design (FR: 80%, R: 3.0 mm) and the proposed die design (FR: 95%, R: 3.0 mm). Figures 11 (a) through to 11(c) show the initial billet and the resulting products of each step.

These experiments were initially conducted to investigate how design changes affect crack defects. In Figs. 12(a) and 12(b), a photograph of the screw head for the initial forging conditions (FR: 80%, R: 3.0 mm) is compared with a photograph of the proposed forging conditions (FR: 95%, R: 3.0 mm). Figure 12(a) reveals microcracks around the six concave regions of the Torx pattern. In contrast, Fig. 12(b) confirms a complete absence of cracks for the proposed conditions.

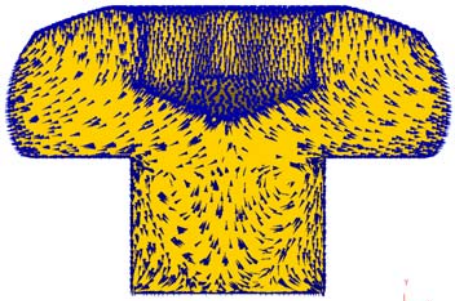

(a) Folding defects (FR = 80%, R = 3.0 mm)

(b) Without folding defects (FR = 95%, R = 3.0 mm)

Fig. 10 Comparison of material flows for the case

(a) (b) (c)

Fig. 11 Experimental results for the multistep forging: (a) the initial billet, (b) the intermediate preform and (c) the final product

Through these experiments, the effect of the design change on the crack defect is investigated at first. Figures 11(a) and (b) compare photographs of the screw head for the initial forging conditions (FR: 80%, R: 3.0 mm) and the proposed forging conditions (FR: 95%, R: 3.0 mm), respectively. It can be seen that micro-cracks were observed around the six concave region of the Torx pattern, as shown in Fig. 11(a). In contrast, those cracks were completely removed when the proposed condition was applied as shown in Fig. 11(b).

The results of the folding defects were also investigated. Figure 12 compares photographs of the inside part of the Torx pattern where folding defects frequently occur frequently. The photograph in Fig. 13(a) shows a folding defect that formed inside the Torx pattern under the initial forging conditions. In contrast, the photograph in Fig. 13(b) shows that no folding defect was formed

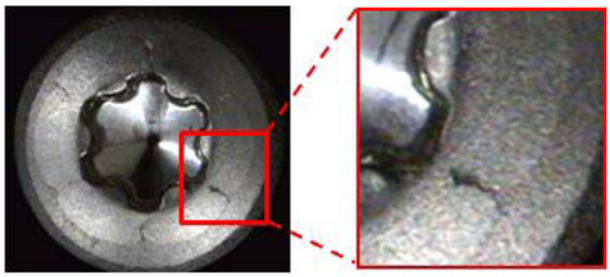

(a) The initial conditions (FR = 80%, R = 3.0 mm)

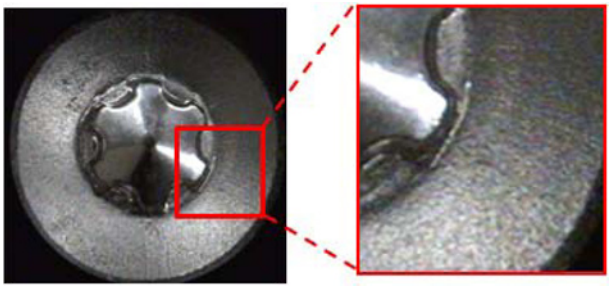

(b) The proposed conditions (FR = 95%, R = 3.0 mm)

Fig. 12 Comparison of the crack on the head surface

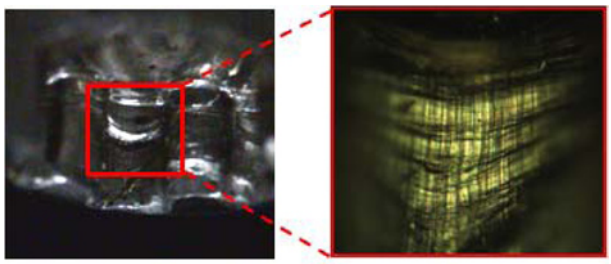

(a) The initial conditions (FR = 80%, R = 3.0 mm)

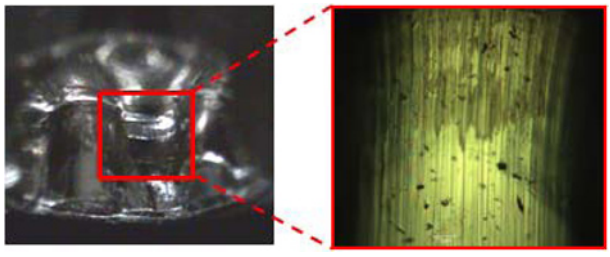

(b) The proposed conditions (FR = 95%, R = 3.0 mm)

Fig. 13 Comparison of the folding defect inside the Torx patterns

under the proposed forging condition. Thus, our FE analyses confirms that the proposed approach can prevent the formation of microcracks by reducing the damage value and by selecting optimal die design parameters.

5. Conclusions

In this study, FE analyses were performed to investigate two types of defects (cracks and folding) which can be generated during the head forging process of subminiature Torx screws. The cracks on the screw head were predicted on the basis of the Cockcroft-Latham damage values. The estimated Cockcroft-Latham damage values were used to select a better preform shape, particularly with respect to crack initiation. The results of the FE analysis of the head forging process show that the damage value decreases as the FR increases and as the corner radius of the upper preform die decreases. When the FR was changed from 80% to 95% and the corner radius was changed from 1.5 mm to 3.0 mm, the damage value at the corner region of the Torx pattern decreased by 43%.

A parametric study was conducted to determine how folding defects can be prevented from forming near the six inside corners of the Torx pattern. Our results confirmed that the FR has a great effect on folding defects, whereas the corner radius has no significant effect on folding defects. No folding defect was expected when the FR value was 95%.

Experiments based on the analysis results were conducted on the original die and the improved die. The results confirm that the improved die can be used to prevent the formation of crack defects and folding defects.

ACKNOWLEDGEMENT

This research was financially supported by the Ministry of Knowledge Economy (MKE) and Korea Institute for Advancement of Technology (KIAT) through the Workforce Development Program in Strategic Technology. The authors would like to thank Dr. Rha of Seoul Metal Co. for his support on the screw forging experiments.

REFERENCES

1. Kong, Y.-K., Lowe, B. D., Lee, S.-J., and Krieg, E. F., "Evaluation of handle shapes for screwdriving," Applied Ergonomics, Vol. 39, No. 2, pp. 191-198, 2008.
2. Seo, W. S., Min, B. W., Park, K., Ra, S. W., Lee, S. H., Kim, J. H., and Kim, J. B., "Design of cold heading process of a screw for storage parts," Trans. Mater. Process., Vol. 20, No. 1, pp. 48-53, 2011.
3. Mackerle, J., "Finite element modelling and simulation of bulk material forming: A bibliography (1996-2005)," Eng. Comput., Vol. 23, No. 3, pp. 250-342, 2006.
4. Cha, D. J., Kim, D. K., Cho, J. R., and Bae, W. B., "Hot shape forging of gas turbine disk using microstructure prediction and finite element analysis," Int. J. Precis. Eng. Manuf., Vol. 12, No. 2, pp. 331-336, 2011.
5. Lee, Y. K. and Yang, D. Y., "Development of a grid-based mesh generation technique and its application to remeshing during the finite element simulation of a metal forming process," Eng. Comput., Vol. 16, No. 3, pp. 316-339, 1999.
6. Behrens, A. and Just, H., "Verification of the damage model of effective stresses in cold and warm forging operations by experimental testing and FE simulations," J. Mater. Process. Technol., Vol. 125-126, pp. 295-301, 2002.
7. Kubota, S., Yamamoto, T., and Yamanaka, M., "Forging process design by the computer simulation," Trans. Mater. Process., Vol. 16, No. 2, pp. 95-100, 2007.
8. Chen, J. and Young, B., "Stress–strain curves for stainless steel at elevated temperatures," Eng. Struct., Vol. 28, No. 2, pp. 229-239, 2006.
9. Cockcroft, M. G. and Latham, D. H., "Ductility and the workability of metals," J. Inst. Metals, Vol. 96, pp. 33-39, 1968.